Foster, D. M., Jacquez, J. A., Lieb, W. R., & Stein, W. D. (1979) *Biochim. Biophys. Acta 555*, 349–351.
Ginsburg, H., & Stein, W. D. (1975) *Biochim. Biophys. Acta 382*, 353–368.
Gorga, F. R., & Lienhard, G. E. (1981) *Biochemistry 20*, 5108–5113.
Hankin, B. L., Lieb, W. R., & Stein, W. D. (1972) *Biochim. Biophys. Acta 288*, 114–126.
Harris, E. J. (1964) *J. Physiol. (London) 173*, 344–353.
Harris, J. W., & Kellermeyer, R. W. (1970) *The Red Cell*, Harvard University Press, Cambridge, MA.
Helgerson, A. L., & Carruthers, A. (1987) *J. Biol. Chem. 262*, 5464–5475.
Holman, G. D., & Rees, W. D. (1987) *Biochim. Biophys. Acta 897*, 395–405.
Jensen, M. R., & Brahm, J. (1987) *Biochim. Biophys. Acta 900*, 282–290.
Jung, C. Y. (1975) in *The Red Blood Cell* (Surgenor, D. M., Ed.) 2nd ed., pp 705–751, Academic Press, New York.
Karlish, S. J. D., Lieb, W. R., Ram, D., & Stein, W. D. (1972) *Biochim. Biophys. Acta 255*, 126–132.
Lacko, L., Wittke, B., & Kromphardt, H. (1972) *Eur. J. Biochem. 25*, 447–454.
Lieb, W. R., & Stein, W. D. (1977) *J. Theor. Biol. 69*, 311–319.
Lin, S., & Snyder, C. E., Jr. (1977) *J. Biol. Chem. 252*, 5464–5471.
Lowe, A. G., & Walmsley, A. R. (1986) *Biochim. Biophys. Acta 857*, 146–159.
Miller, D. M. (1968) *Biophys. J. 8*, 1339–1352.
Miller, D. M. (1971) *Biophys. J. 11*, 915–923.
Mueckler, M., Caruso, C., Baldwin, S. A., Panico, M., Blench, I., Morris, H. R., Allard, W. J., Lienhard, G. E., & Lodish, H. F. (1985) *Science (Washington, D.C.) 229*, 941–945.
Naftalin, R. J., & Holman, G. D. (1977) in *Membrane Transport in Red Cells* (Ellory, J. C., & Lew, V. L., Eds.) pp 257–300, Academic Press, New York.
Naftalin, R. J., Smith, P. M., & Roselaar, S. E. (1985) *Biochim. Biophys. Acta 820*, 235–239.
Rees, W. D., & Gliemann, J. (1985) *Biochim. Biophys. Acta 812*, 98–106.
Regen, D. M., & Morgan, H. E. (1964) *Biochim. Biophys. Acta 79*, 151–161.
Sen, A. K., & Widdas, W. F. (1962) *J. Physiol. (London) 160*, 392–403.
Sogin, D. C., & Hinkle, P. C. (1980) *Biochemistry 19*, 5417–5420.
Stein, W. D. (1986) *Transport and Diffusion across Cell Membranes*, Academic Press, Orlando, FL.
Vidaver, G. A. (1966) *J. Theor. Biol. 10*, 301–306.
Wang, J.-F., Falke, J. J., & Chan, S. I. (1986) *Proc. Natl. Acad. Sci. U.S.A. 83*, 3277–3281.
Weiser, M. B., Razin, M., & Stein, W. D. (1983) *Biochim. Biophys. Acta 727*, 379–388.
Wheeler, T. J. (1986) *Biochim. Biophys. Acta 862*, 387–398.
Wheeler, T. J., & Hinkle, P. C. (1985) *Annu. Rev. Physiol. 47*, 503–517.
Wheeler, T. J., & Whelan, J. D. (1987) *Fed. Proc., Fed. Am. Soc. Exp. Biol. 46*, 1982.
Widdas, W. F. (1980) *Curr. Top. Membr. Transp. 14*, 165–223.

Lateral Diffusion and Fluorescence Microscope Studies on a Monoclonal Antibody Specifically Bound to Supported Phospholipid Bilayers

Lukas K. Tamm
Department of Biophysical Chemistry, Biocenter, University of Basel, CH-4056 Basel, Switzerland
Received July 21, 1987; Revised Manuscript Received October 26, 1987

ABSTRACT: Supported phospholipid bilayers prepared by Langmuir–Blodgett techniques were introduced recently as a new model membrane system [Tamm, L. K., & McConnell, H. M. (1985) *Biophys. J. 47*, 105–113]. Here, supported bilayers are applied to study the lateral diffusion and lateral distribution of membrane-bound monoclonal antibodies. A monoclonal anti-trinitrophenol antibody was found to bind strongly and with high specificity to supported phospholipid bilayers containing the lipid hapten (trinitrophenyl)phosphatidylethanolamine at various mole fractions. The lateral distribution of the membrane-bound antibodies was studied by epifluorescence microscopy. The bound antibodies aggregated into patches on a host lipid bilayer of dimyristoylphosphatidylcholine below the lipid chain melting phase transition and redistributed uniformly on fluid-phase supported bilayers. Lateral diffusion coefficients and mobile fractions of fluorescent phospholipid analogues and fluorescein-labeled antibodies were measured by fluorescence recovery after pattern photobleaching. The lateral diffusion coefficients of the membrane-bound antibodies resembled those of the phospholipids but were reduced by a factor of 2 in the fluid phase. The lipid chain melting phase transition was also reflected in the lateral diffusion coefficient of the bound antibody but occurred at a temperature about 3 deg higher than the phase transition in supported bilayers of pure phospholipids. The antibody lateral diffusion coefficients decreased in titration experiments monotonically with increasing antibody surface concentrations by a factor of 2–3. Correspondingly, a relatively small decrease of the antibody lateral diffusion coefficient was observed with increasing mole fractions of lipid haptens in the supported bilayer.

Model membranes have often proven to be very useful for obtaining detailed information on many physical and functional properties of biological membranes. Interactions between lipids and proteins, the binding of water-soluble molecules and ions, and membrane transport phenomena have been studied in various model membrane systems with much success. How-

0006-2960/88/0427-1450$01.50/0

ever, several processes in biology—such as, for instance, the activation of lymphocytes, the infection of cells by viruses, or the intracellular membrane recycling—require a physical contact between two different membranes. Although they are biologically very important, interactions between different membranes are still characterized quite insufficiently in molecular terms, and mainly for technical reasons, it is still very difficult to assess the structural and dynamical properties of the molecules participating at the site of the membrane–membrane contact. In order to overcome some of these difficulties, planar supported model membranes have been designed and introduced recently by McConnell and co-workers [for a review see McConnell et al. (1986)]. The planar supported membranes are ideally suited for optical studies of reactions at membrane–water interfaces, for lateral diffusion measurements of surface-bound molecules, or for study of the receptor-mediated binding of cells to the model membrane.

In the earlier work of Hafeman et al. (1981), phospholipid monolayers containing lipid hapten were supported on alkylated coverslips. When macrophages were bound the supported monolayers via their F_c receptors and a specific antibody, they were stimulated to release superoxide and the lysosomal enzyme cathepsin B, two typical cytotoxic response reactions of macrophages in vivo. Supported monolayers, however, model only half of a biological bilayer membrane correctly and, hence, are not appropriate for many membrane studies, for example, those that require the successful reconstitution of integral membrane proteins. Having this in mind, supported phospholipid bilayers have recently been developed and used as a new planar model membrane system (Tamm & McConnell, 1985). For the preparation of supported bilayers, two monolayers were sequentially transferred from the air–water interface of a Langmuir trough onto hydrophilic supports. Measurements of the lipid lateral diffusion coefficients showed that (i) these membranes were large and continuous, (ii) the lateral mobilities were very similar to those measured in liposomes, and (iii) sharp lipid-phase transitions could be observed in this system just as in liposomes.

In the present study, supported bilayers have been used in an initial application to measure the lateral diffusion and distribution of a peripheral "membrane" protein, namely, a monoclonal antibody. This antibody (IgG)[1] is bivalent and binds specifically to lipid haptens which have been included into supported bilayers of DMPC at various mole fractions. The effect of the phospholipid phase transition on the lateral distribution and diffusion of the bound antibodies and the dependence of the lateral diffusion coefficients on the surface concentration of bound antibodies are described here.

Materials and Methods

Lipids. All phospholipids, lipid haptens, and fluorescent phospholipid analogues were from Avanti Polar Lipids, shown to be pure by silica gel thin-layer chromatography, and used without further purification.

Antibodies. The anti-TNP IgG-producing mouse hybridoma cell line GK14-1 was a kind gift of Dr. G. Köhler (University of Freiburg, F.R.G.). The antibodies (subclass γ_{2b},κ) were purified and labeled according to standard procedures (Goding, 1983; Forni, 1979). Briefly, ascites fluid or cell culture supernatant was precipitated with $(NH_4)_2SO_4$ (30–50% and 0–60% saturation fractions were used, respectively). The precipitated protein was dissolved in 50 mM Tris-HCl, pH 8.2, containing 0.15 M NaCl, dialyzed, and affinity purified on a protein A–Sepharose CL-4B column (Pharmacia). The IgG fraction was eluted with 50 mM sodium citrate, pH 3.5, containing 0.15 M NaCl and shown to be pure by SDS–polyacrylamide gel electrophoresis (Laemmli, 1970). Protein concentrations were determined by the method of Lowry et al. (1951) with BSA as a standard. Specific binding activities to TNP-BSA (2 mol/mol) (Kiefer, 1979) were monitored with ELISA tests (Douillard & Hoffmann, 1983). In well-purified preparations we obtained half-maximal ELISA signals at antibody concentrations of 20–30 ng/mL. Typical yields were 5.6 mg of IgG/mL of ascites fluid and 13.4 mg of IgG/L of culture supernatant. FITC (Molecular Probes) was coupled at 50 μg of FITC/mg of protein and 3–5 mg/mL of protein in 50 mM sodium carbonate, pH 9.2, containing 0.15 M NaCl, and unreacted FITC was removed on a Sephadex G-25 gel filtration column that was equilibrated with PBS. The resulting molar ratios of fluorescein-to-protein were 1.1–1.3. Labeling did not have any adverse effect on the binding activity as judged by the ELISA.

Substrates. p111 and n100 silicon wafers (3-in. diameter) were obtained from Aurel GmbH, Landsberg, F.R.G. A SiO_2 layer of 100 nm was thermally grown in an oxidizing atmosphere at CSEM, Neuchâtel, Switzerland. The wafers were cut into pieces of about 5 cm^2, boiled for 10 min in 10% contrad 90 cleaning solution (Technosa, Lausanne, Switzerland), sonicated for 30 min in a bath sonicator, and rinsed extensively with distilled water. Subsequently they were treated with oxidizing base and acid and HF as described (Tamm & McConnell, 1985). The wafers were cleaned in a plasma cleaner (Harrick Scientific Corp.) under argon for 10 min immediately before the monolayers were transferred.

Supported Bilayers. The phospholipids were spread from hexane–ethanol (9:1) solutions on two different Langmuir troughs: Trough 1 was a commercial and fully automated circular multicompartment trough (Mayer Feintechnik, Göttingen, F.R.G.) and was equipped with an automatic film lift (Fromherz, 1975). Trough 2 was home-built, rhombus-shaped, and similar to that described by von Tscharner and McConnell (1981). The surface pressures on both troughs were measured by the Wilhelmy method with linear transducers (SS-101, Collins Corp.) and with plates cut from Whatman No. 1 filter paper. Both troughs were placed in a vibration-damped, "dust-free" bench-top cabinet.

Phospholipid monolayers were compressed to 36 mN/m in both troughs on subphases of quartz-distilled and ion-exchanged water. Clean wafers were rapidly and vertically immersed through the compressed monolayer on trough 1 with the automatic film lift. The surface pressure dropped only very little and was readjusted to the original 36 mN/m. The wafer was then slowly (5 mm/min) withdrawn while the surface pressure was maintained constant at 36 mN/m by adjusting the surface area of the monolayer with the electronic feedback circuit. One phospholipid monolayer was deposited on both sides of the wafer as judged from the area loss of the monolayer

[1] Abbreviations: BSA, bovine serum albumin; DMPC, 1,2-dimyristoyl-3-*sn*-phosphatidylcholine; ELISA, enzyme-linked immunosorbent assay; FITC, fluoresceinyl isothiocyanate; FRAP, fluorescence recovery after pattern photobleaching; IgG, immunoglobulin G; NBD-DMPE, *N*-(7-nitro-2,1,3-benzoxadiazol-4-yl)-1,2-dimyristoyl-3-*sn*-phosphatidylethanolamine; NBD-eggPE, egg *N*-(7-nitro-2,1,3-benzoxadiazol-4-yl)phosphatidylethanolamine; NBD-PC, 1-acyl-2-[6-[(7-nitro-2,1,3-benzoxadiazol-4-yl)amino]caproyl]phosphatidylcholine; PBS, phosphate-buffered saline (10 mM sodium phosphate, pH 7.4, 0.15 M NaCl); PIPES, piperazine-*N*,*N*'-bis(2-ethanesulfonic acid); POPC, 1-palmitoyl-2-oleoyl-3-*sn*-phosphatidylcholine; Rh-DOPE, *N*-(lissamine rhodamine B sulfonyl)-1,2-dioleoyl-3-*sn*-phosphatidylethanolamine; SDS, sodium dodecyl sulfate; TNP, 2,4,6-trinitrophenol; TNP-cap-eggPE, egg *N*-[[(2,4,6-trinitrophenyl)amino]caproyl]phosphatidylethanolamine; Tris-HCl, tris(hydroxymethyl)aminomethane hydrochloride.

on the trough: twice the area of the wafer was removed from the trough. The coated substrate was then attached horizontally to another lift on trough 2, slowly lowered until it contacted the interface with the compressed monolayer (36 mN/m), left approximately 10 s for equilibration, and finally pushed through the interface. Again, an area equivalent to the surface of the substrate was removed from the monolayer trough, and a single planar, phospholipid bilayer was formed on the lower side of the substrate (Tamm & McConnell, 1985). The wafer with the bilayer was then mounted with double-stick tape in a plastic Petri dish which had a glass coverslip bottom (see Figure 1) and which was previously placed underneath monolayer 2. The supported bilayer was never exposed to air during all subsequent manipulations. The sample assembly was withdrawn from the Langmuir trough and ready for lipid diffusion measurements.

For the experiments with antibodies, the water was exchanged with PBS by flowing an excess through the narrow space between the membrane and the coverslip. The bilayer was then incubated with the appropriate concentration of fluorescein-labeled IgG in 200 μL of PBS for 5 min. Unbound antibody was subsequently washed away with an excess of PBS.

Lateral Diffusion Measurements. Lateral diffusion coefficients and mobile fractions were measured by monitoring the fluorescence recovery after pattern photobleaching (FRAP) (Smith & McConnell, 1978).

An early version of our FRAP apparatus has been described (Hänggi-Mojtabai, 1985). A brief description of the present instrumentation is given here: The sample on the stage of an inverted epifluorescence microscope (Zeiss, IM-35, F.R.G.) is illuminated by the 488-nm line of a 4-W argon ion laser (Innova 70-4, Coherent). Prebleach, bleach, and observe pulses are generated by an acoustooptic modulator (AOM-40, Intra Action) which is controlled by an Apple II microcomputer. The first-order diffracted beam is optically selected, expanded, and directed into the microscope through a Ronchi ruling (Edmund Scientific) which has been positioned in an image plane external to the microscope. The fluorescence emission is collected in the photometer head, and the photomultiplier tube output is recorded on a Datalab transient recorder (DL 905, Datalab). The transient recorder is interfaced to the Apple II microcomputer, which also controls an electronic shutter (Uniblitz, Vincent). The shutter has been built into the fluorescence emission path in the microscope and is closed during the bleach pulse for protection of the photomultiplier tube.

Normally, a 40× water-immersion objective (0.75 N.A., Zeiss) was used, which illuminated a sample area of about 20 000 μm^2. In a typical experiment, one prebleach pulse of 60-ms duration was followed by one 30–40-ms bleach pulse and a trace of 40 observation pulses of 40 ms each. The intensity of the prebleach and the observation pulses was about 800 times lower than that of the bleach pulse, and no significant additional photobleaching was observed during data collection. The supported bilayer membranes were mounted on a special sample assembly holder on the stage of the microscope and were temperature controlled with a Peltier element (Figure 1). The temperature was measured with a digital thermometer (Fluke, Model 2190A, Holland) with a miniature thermocouple which was placed at the upper surface of the wafer. The precision of the temperature control was ±0.1 deg and a systematic error in measuring the actual bilayer temperature is believed to be less than ±0.5 deg.

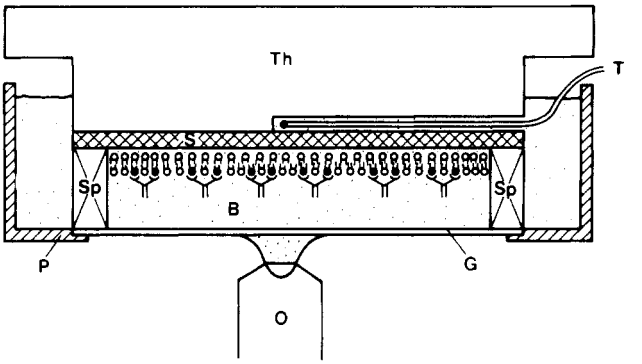

FIGURE 1: Sample assembly and experimental set-up for epifluorescence microscopy and lateral diffusion measurements. Supported bilayer and substrate (S) are mounted with spacers (Sp) in a Petri dish (P) with a thin glass coverslip window (G). The sample is temperature controlled with a thermoelectric Peltier element (Th), and the sample temperature is measured with a thermocouple (T). A long-distance water-immersion objective (O) attached to an inverted microscope is used to view the sample by epifluorescence microscopy and to measure lateral diffusion. In all experiments with antibodies the aqueous phase was phosphate-buffered saline at pH 7.4 (B). (Figure not drawn to scale.)

The raw fluorescence recovery data were evaluated on the Apple II computer by a nonlinear least-squares Marquart fit to a single exponential (Gaupp et al., 1980). The three free-fit parameters (time constant, amplitude, and end value) were determined, and from these the diffusion coefficients and mobile fractions were calculated. The fits to a single exponential were usually very good with an error of the time constant of less than 10% in individual experiments. Typically, the results of three to five individually fitted bleach experiments were averaged and yielded standard deviations of less than 10% in most cases in single bilayers (see also Table I).

Microphotography. Epifluorescence microscope photographs were taken with an Olympus OM-2 camera attached to the IM-35 on Ilford HP5 1000 ASA photographic film. The film was exposed for about 2 s at a low laser illumination intensity and push processed with Ilford Microphen developer.

Fluorescence Binding Assay. A detailed description of this binding assay will be given elsewhere. Briefly: two solutions of fluorescein-labeled antibodies (31.3 nM) in 10 mM PIPES, pH 7.4, containing 0.15 M NaCl were titrated in parallel with identical amounts of vesicles. Small unilamellar vesicles were made by sonication on a MSE tip sonicator under argon for 10 min at 30 °C. Vesicles which were 5 mM in DMPC and which contained 1 mol % TNP-cap-eggPE and 5 mol % Rh-DOPE were titrated into the first cuvette, and vesicles that were identical, except that Rh-DOPE had been omitted, were titrated into the second cuvette. Fluorescence was measured at 25 °C on a Schoeffel RRS 1000 fluorometer. Excitation was at 480 nm, and the fluorescence emission was recorded at 513 nm. The binding parameter b was calculated according to eq 1, where F_0^{Rh} and F_0^{Ves} are the antibody fluorescence

$$b = \frac{F^{Ves}}{F_0^{Ves}} - \frac{F^{Rh}}{F_0^{Rh}} \quad (1)$$

intensities before the vesicles with and without Rh-DOPE, respectively, were titrated and F^{Rh} and F^{Ves} are the respective fluorescence intensities at each titration point.

RESULTS

The monoclonal antibody (IgG) GK14-1 was originally raised and selected for binding to TNP-derivatized surface antigens of sheep red blood cells. Figure 2 shows that the purified and fluorescein-labeled antibody also binds to artificial

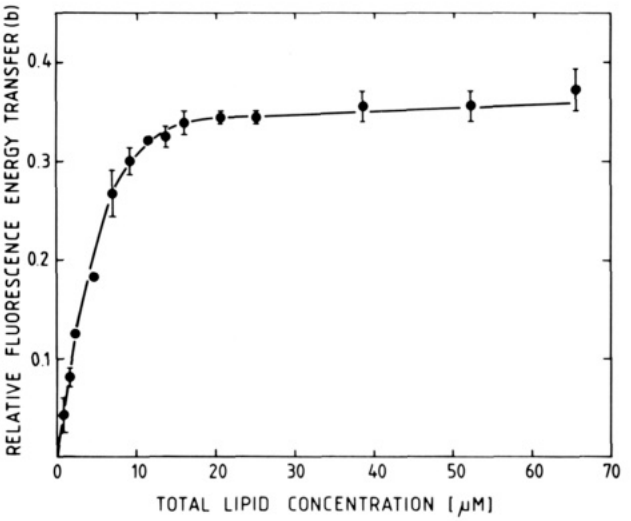

FIGURE 2: Binding of fluorescein-labeled monoclonal anti-TNP antibodies to small unilamellar DMPC vesicles containing 1 mol % TNP-cap-eggPE. The binding was determined by measuring the relative fluorescence energy transfer from fluorescein to rhodamine B, which was also included in the membranes (see Materials and Methods). The vesicles were titrated to a 31.3 nM solution of IgG in 10 mM PIPES, pH 7.4, at 25 °C.

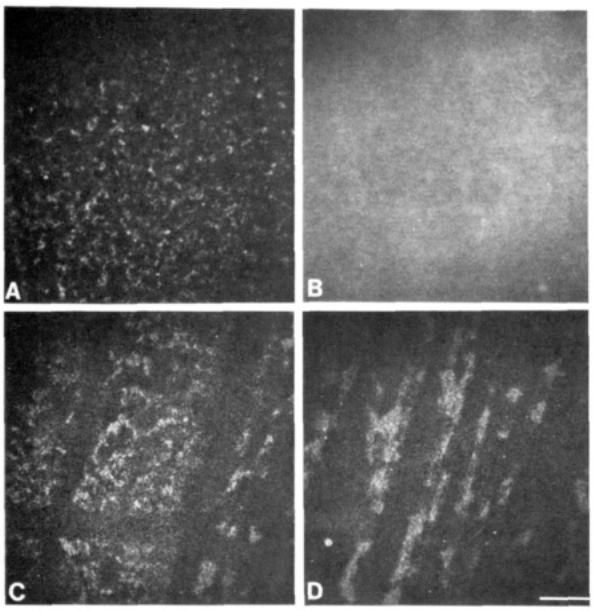

FIGURE 3: Epifluorescence microscope photographs showing the reversible patching of antibody–lipid hapten complexes upon the phospholipid phase transition in supported bilayers. A supported bilayer composed of DMPC plus 5 mol % TNP-cap-eggPE in the leaflet facing the large aqueous compartment was incubated with 5 μg/mL fluorescent monoclonal anti-TNP antibody for 5 min. The photographs were taken at 20 °C shortly after incubation (A), at 30 °C (B), at 20 °C after cooling from 30 °C (C), and at 25 °C on the following day (D). Photographs A, C, and D show patches consisting of lipid hapten domains with bound fluorescent antibodies. These domains are phase separated from DMPC and increase in size from (A) to (D). At 30 °C (B) the membrane is monophasic, fluid, and uniformly stained with antibodies. (The bar represents 30 μm.)

membrane vesicles composed of DMPC plus 1 mol % TNP-cap-eggPE and 5 mol % Rh-DOPE very specifically. Since our binding assay is based on the fluorescence energy transfer from fluorescein (antibody) to rhodamine (vesicle surface), which can occur only over short distances (≤50–80 Å), only the bound antibodies contribute to the observed quenching signal defined by eq 1. A Scatchard analysis of the binding curve in Figure 2 yielded at 25 °C an apparent binding constant of $(2.2 \pm 0.5) \times 10^8$ with 1.9 ± 0.1 lipid haptens bound

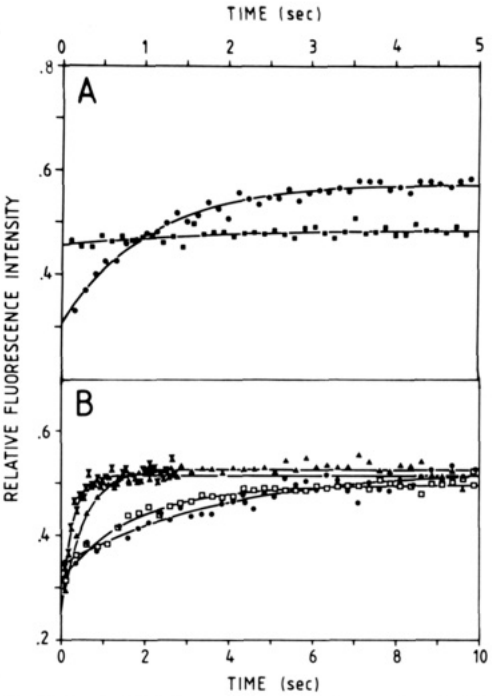

FIGURE 4: Lateral diffusion measurements on phospholipids and antibodies in single planar supported bilayers. (A) Fluorescence recovery after pattern photobleaching in a single planar DMPC bilayer containing 2 mol % NBD-DMPE in both leaflets at 10 (■) and 30 °C (●). The periodicity of the Ronchi ruling on the membrane was 12.7 μm. The data at 30 °C were fit to a single exponential (curve) which yielded a lateral diffusion coefficient of $(3.8 \pm 0.2) \times 10^{-8}$ cm²/s and a mobile fraction of 79%. (B) FRAP curves of asymmetric bilayers [DMPC in the leaflet facing the substrate; DMPC/TNP-cap-eggPE (1:1) in the leaflet facing the large aqueous compartment] to which 20 μg/mL fluorescein-labeled monoclonal anti-TNP IgG was allowed to bind for 5 min. The periodicity of the Ronchi ruling on the membrane was 2.5 μm. The following diffusion parameters were derived from fits to single exponentials: (●) 10 °C, $(4.9 \pm 1.0) \times 10^{-10}$ cm²/s, 56 ± 4%; (□) 15 °C, $(1.4 \pm 0.5) \times 10^{-9}$ cm²/s, 60 ± 4%; (▲) 20 °C, $(6.0 \pm 0.8) \times 10^{-9}$ cm²/s, 72 ± 7%; (solid hourglass) 25 °C, $(1.1 \pm 0.05) \times 10^{-8}$ cm²/s, 74 ± 2%.

to each antibody at saturation. Strong specific binding was also observed to planar supported bilayers of DMPC containing the lipid hapten (TNP-cap-eggPE) at various mole fractions as judged from the increase in fluorescence intensity (data not shown). No significant binding to phospholipid vesicles or supported bilayers occurred in the absence of lipid hapten or with an unspecific antibody.

The lateral distribution of antibodies bound to supported phospholipid bilayers was examined by epifluorescence microscopy (Figure 3). The antibody distribution on supported DMPC bilayers with 5 mol % lipid hapten included in the second (antibody facing) monolayer was polymorphic: below the chain melting phase transition of DMPC the antibodies clustered into small domains (Figure 3A) which disappeared above the phase transition on the uniformly stained, liquid-crystalline membrane (Figure 3B). This process was reversible, and the antibody domains grew in size upon prolonged incubation time (Figure 3C,D).

It has been shown earlier (Tamm & McConnell, 1985) that single planar bilayers could be assembled on carefully cleaned hydrophilic surfaces and that the phospholipids in these model membranes showed rapid lateral mobilities, comparable to those measured in liposome preparations or cell membranes. In order to illustrate the performance of our new FRAP instrument and the signal-to-noise ratio achievable by periodic pattern photobleaching on single supported phospholipid bilayers, a few typical FRAP curves are shown in Figure 4.

Table I: Lateral Diffusion Coefficients and Mobile Fractions of Lipids and Antibodies in Planar Supported Bilayers and Multibilayers[a]

	15 °C		20 °C		30 °C	
	D ($\mu m^2/s$)[b]	mf (%)[c]	D ($\mu m^2/s$)	mf (%)	D ($\mu m^2/s$)	mf (%)
(1) DMPC multibilayers: 0.5 mol % NBD-eggPE	$<10^{-2}$		$<10^{-2}$		6.35 ± 0.76	97.4 ± 2.6
(2) eggPC multibilayers: 0.5 mol % NBD-eggPE	5.43 ± 0.31	85.4 ± 6.0	6.43 ± 0.21	81.8 ± 7.0	10.46 ± 0.49	86.4 ± 3.2
(3) DMPC bilayer: 2 mol % NBD-eggPE (B)	$<10^{-2}$		0.66 ± 0.02	63.8 ± 3.8	3.75 ± 0.40	81.8 ± 8.0
(4) DMPC bilayer: 4 mol % NBD-eggPE (S)					3.67 ± 0.22	80.0 ± 3.0
(5) DMPC bilayer: 4 mol % NBD-eggPE (A)					3.85 ± 0.28	82.6 ± 5.6
(6) DMPC bilayer: 2 mol % NBD-DMPE (A)	$<10^{-2}$		0.94 ± 0.27	75.6 ± 7.0	3.20 ± 0.59	74.8 ± 0.6
(7) POPC bilayer: 2 mol % NBD-eggPE (B)	2.39 ± 0.08	72.6 ± 1.2	2.92 ± 0.19	76.8 ± 1.8	4.57 ± 0.10	75.2 ± 3.8
(8) POPC bilayer: 2 mol % NBD-PC(C-6) (B)	2.33 ± 0.19	47.8 ± 2.2	2.61 ± 0.49	49.2 ± 2.0	2.95 ± 0.10	49.2 ± 2.6
(9) DMPC bilayer + 0.15 M NaCl: 2 mol % NBD-eggPE (B)					3.97 ± 0.20	81.2 ± 1.4
(10) DMPC bilayer + 10 mM $CaCl_2$: 2 mol % NBD-eggPE (B)					3.29 ± 0.18	74.4 ± 4.8
(11) DMPC bilayer: 5 mol % TNP-cap-PE (A), 20 μg/mL GK14-1	$<10^{-2}$		0.038 ± 0.014	54.2 ± 5.4	2.01 ± 0.27	93.8 ± 8.0

[a] B = both leaflets of the bilayer are labeled. S = only the leaflet facing the substrate is labeled. A = only the leaflet facing the large aqueous compartement is labeled. [b] Diffusion coefficient (1 $\mu m^2/s = 10^{-8}$ cm^2/s). [c] Mobile fraction.

Figure 4A shows two FRAP curves obtained from a single silicon supported DMPC bilayer at 10 (squares) and at 30 °C (dots), respectively. Both leaflets of this bilayer were labeled with 2 mol % NBD-DMPE, and the relative fluorescence intensity of the membrane before bleaching was 1.0. A diffusion coefficient of $(3.8 \pm 0.2) \times 10^{-8}$ cm^2/s with a mobile fraction of 79%[2] was calculated from a nonlinear least-squares fit of the recovery data at 30 °C to a single exponential (continuous curve). This clearly indicated that most of the fluorescent lipid analogues in both leaflets of the supported bilayer were mobile and that, most probably, a thin aqueous compartment existed between the bilayer and the substrate as noted already earlier (Tamm & McConnell, 1985). The supported DMPC membrane at 10 °C showed no recovery and was immobile on a time scale down to 10^{-10} cm^2/s. Several FRAP curves of fluorescein-labeled antibodies which were bound to supported phospholipid bilayers are depicted in Figure 4B. This membrane was 100% DMPC in the first monolayer (facing the substrate) and 1:1 DMPC/TNP-cap-eggPE in the second monolayer (facing the large aqueous compartment). Labeled antibodies were allowed to bind to the supported bilayer in PBS at a concentration of 20 μg/mL for 5 min before unbound antibodies were washed away with an excess of PBS. The FRAP curves were taken at increasing temperatures, 10, 15, 20, and 25 °C, and showed increasing diffusion coefficients and mobile fractions (see figure legend). Note that the time scales and the periodicities of the periodic pattern are different in panels A and B of Figure 4.

A summary of several lateral diffusion measurements of lipids and antibodies is given in Table I. The first two rows summarize data obtained with conventional multibilayer preparations [prepared as in Rubenstein et al. (1979)]. These measurements were performed in order to calibrate our FRAP apparatus and to compare our results with earlier measurements of other groups. In fact, the agreement between our measurements and the results obtained in other laboratories on identical systems is very good (Rubenstein et al., 1979; Criado et al., 1982; Wu et al., 1977).[3] The lateral diffusion coefficients and the mobile fractions obtained from measurements on single DMPC bilayers supported on oxidized silicon (row 3) were reduced by about 40% and about 16%, respectively, when compared to the DMPC multibilayers with the same probe. Rows 4 and 5 show that the diffusion coefficients and the mobile fractions of NBD-eggPE in DMPC were the same, when the bilayers were labeled asymmetrically, irrespective of whether the label was in the first or second monolayer. This result confirmed the earlier finding that supported bilayers labeled in both leaflets exhibited high mobile fractions and that these FRAP curves were characterized by a single diffusion coefficient (Tamm & McConnell, 1985; see also Figure 4A). It also corroborates the idea of a thin aqueous compartment between the bilayer and its support. Different fluorescent phospholipid analogues diffused at slightly different rates in different host lipid bilayers and depended on whether the NBD label was attached to the head group or one of the fatty acyl chains of the phospholipid (rows 6–8). A similar behavior is known from lateral diffusion measurements on multibilayers (Vaz & Hallmann, 1985). Rows 9 and 10 demonstrate that mono- and divalent cations had little or no effect on the lipid diffusion in supported bilayers. The last row in Table I shows the diffusion data of the fluorescein-labeled antibody bound to a supported DMPC bilayer. The lateral diffusion coefficient of the surface bound antibody was reduced by a factor of 2 (from 3.9×10^{-8} to 2.0×10^{-8} cm^2/s) when compared to the lateral diffusion coefficient of the DMPC bilayer labeled with NBD-eggPE and measured at 30 °C.

In an earlier report, sharp phospholipid chain melting phase transitions in supported phospholipid bilayers were observed (Tamm & McConnell, 1985). In this study, I investigated whether the lipid phase transitions were abolished or influenced by the binding of antibodies to the planar lipid bilayer. Melting curves of membranes with different contents of lipid hapten and bound antibody are shown in Figure 5 along with the melting curve of a supported DMPC bilayer but with a lipid label (filled squares) and with the lateral diffusion data of a supported POPC bilayer (filled circles). While the diffusion coefficients in supported POPC bilayers were always high and increased gradually from 2.4×10^{-8} to 5.5×10^{-8} cm^2/s between 15 and 35 °C, sharp phase transitions were observed in the DMPC bilayers with 2 mol % NBD-DMPE or 2 mol % TNP-cap-eggPE and incubated with intermediate levels of fluorescent antibody. The phase transition temperature of the supported bilayer was shifted from 19 °C (the pure lipid-phase transition temperature in supported DMPC

[2] Note: In periodic pattern photobleaching a fluorescence recovery of 50% represents a mobile fraction of 100% [cf. Smith and McConnell (1978)].

[3] The lateral diffusion coefficients of some fluorescein-labeled proteins in solution were also measured by FRAP (F) and showed that there was a very good correlation with the diffusion coefficients obtained by sedimentation (S), e.g., 8.0×10^{-7} cm^2/s (F) vs 7.8×10^{-7} cm^2/s (S) for ovalbumin, 6.4×10^{-7} cm^2/s (F) vs 6.0×10^{-7} cm^2/s (S) for BSA, and 2.7×10^{-7} cm^2/s (F) vs 2.6×10^{-7} cm^2/s (S) for thyroglobulin.

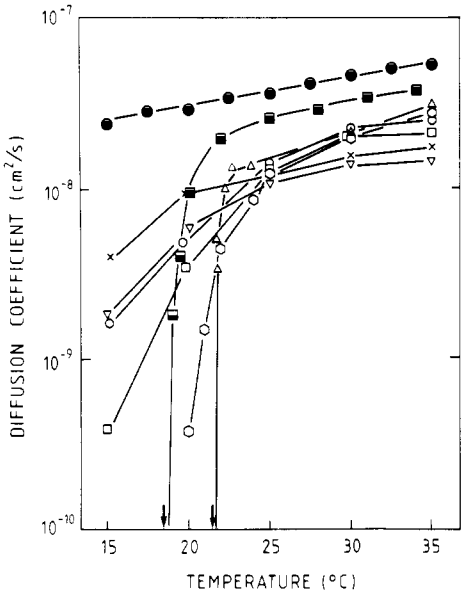

FIGURE 5: Chain melting phase transitions in supported phospholipid bilayers as detected by the lateral diffusion of fluorescent lipid probes (closed and semiclosed symbols) and of fluorescein-labeled monoclonal anti-TNP antibodies (open symbols). (●) POPC plus 2 mol % NBD-eggPE (in both leaflets); (■) DMPC plus 2 mol % NBD-DMPE (in the leaflet facing the large aqueous compartment; the black level in the symbol represents percent mobile fraction of the probe); DMPC plus (△) 2, (○) 5, (□) 10, (○) 25, (▽) 50, and (×) 100 mol % TNP-cap-eggPE (in the leaflet facing the large aqueous compartment) incubated with 20 μg/mL fluorescent antibody for 5 min. The supported bilayers of DMPC show a sharp phase transition at around 19 °C, and the POPC bilayers are fluid (liquid crystalline) in the whole displayed temperature range. The temperature-induced phase transition broadens with increasing amounts of lipid hapten, and the transition temperature is shifted by about 3 deg to higher temperatures in the presence of bound antibodies.

bilayers) to 22 °C in the presence of membrane-bound antibody, probably due to protein–protein interactions at the membrane surface. When the mole fraction of TNP-cap-eggPE was increased up to 100% in the second monolayer, the sharp lipid-phase transition gradually smoothed out and finally disappeared.

One of the original goals of this work was to investigate the influence of protein–protein interactions at the surface of a membrane on their lateral diffusion behavior. In order to find out whether membrane-bound protein at high surface concentrations could account for the reduction in mobility by 2 orders of magnitude often encountered with membrane proteins in cells, when compared to membrane proteins in reconstituted systems, the lateral diffusion coefficients of membrane-bound antibodies were measured as a function of the antibody incubation concentration and, hence, the antibody surface concentration (Figure 6). These experiments were all performed at 30 °C with supported DMPC bilayers containing 5 mol % TNP-cap-eggPE in the second monolayer. The diffusion coefficients decreased about 2-fold from about 2.6×10^{-8} to 1.4×10^{-8} cm²/s in the examined concentration range from 2.5 to 60 μg/mL. At about 50–60 μg/mL the membrane was saturated with antibody, and the fluorescence intensity of the washed membranes did not increase any further with increasing incubation concentrations. The mobile fractions decreased only slightly (80% to 64%) between 2.5 and 60 μg/mL antibody. In a related experiment the lipid hapten concentration was changed, and instead, the antibody concentration and the temperature were held constant at 20 μg/mL and 30 °C, respectively (Figure 7). Again, only a 2-fold decrease in the lateral diffusion coefficients was observed

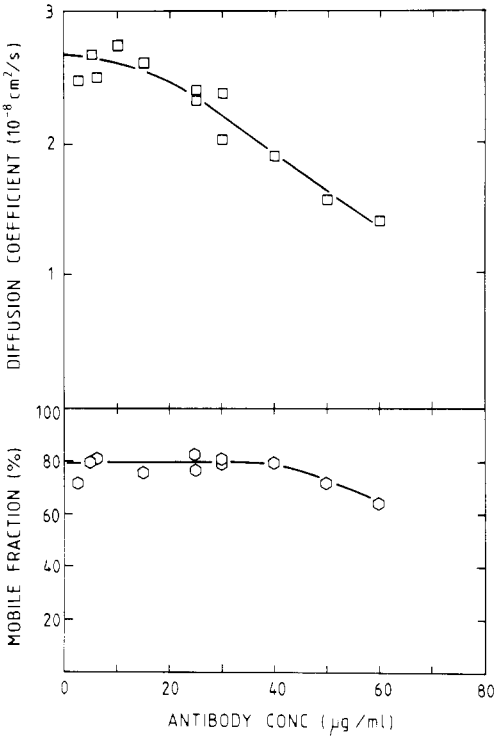

FIGURE 6: Lateral diffusion coefficients and mobile fractions of fluorescent monoclonal anti-TNP antibodies which are specifically bound to supported bilayers composed of DMPC plus 5 mol % TNP-cap-eggPE (in the leaflet facing the large aqueous compartment). The data are plotted as a function of the total antibody concentration during the 5-min incubation period. The measuring temperature was 30 °C.

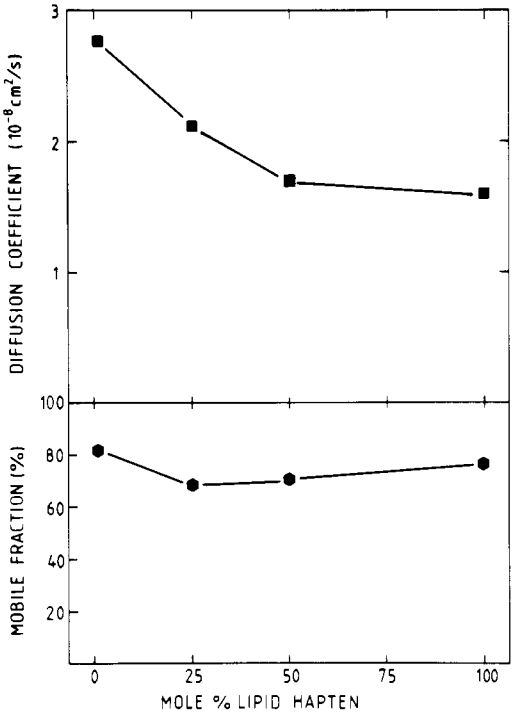

FIGURE 7: Lateral diffusion coefficients and mobile fractions of fluorescent monoclonal anti-TNP antibodies which are specifically bound to supported bilayers composed of DMPC (leaflet facing the substrate) and DMPC/TNP-cap-eggPE at various mole fractions (leaflet facing the large aqueous compartment). Fluorescent monoclonal anti-TNP antibody (20 μg/mL) was allowed to bind for 5 min at all lipid hapten concentrations. The measuring temperature was 30 °C.

with increasing lipid hapten concentrations, and the mobile fractions were always high (70–80%).

Discussion

Lateral heterogeneities at a membrane surface and lateral diffusion measurements of surface-bound membrane proteins have traditionally been difficult to assess in experimental model systems. Either the lateral dimensions of the model system were too small and the membrane curvatures were too high (unilamellar vesicles), or a large number of membranes was stacked with only very thin layers of interstitial water (multibilayers or large coarse liposomes). The supported phospholipid bilayer is a new planar and unilamellar model membrane system that overcomes both of these problems at the same time. Its power is demonstrated in the present work by binding monoclonal antibodies to lipid hapten receptors in the supported membrane and also by showing that lateral phase separations, thermotropic phase transitions, and the effect of the surface density of the protein on the lateral diffusion can be assessed easily.

Lateral phase separations between antibody-rich and antibody-depleted membrane domains are visualized here by epifluorescence microscopy. Before, lateral phase separations have been demonstrated in monolayers by epifluorescence microscopy (Lösche et al., 1983; McConnell et al., 1984) and in bilayers with and without proteins by electron microscopy (Kleemann & McConnell, 1976; Thompson & Tillack, 1985). The antibody lateral diffusion coefficients drop well below 10^{-10} cm^2/s, simultaneously with the reversible and temperature-inducible formation of antibody patches. This behavior observed in our model system parallels patching and the concomitant abrupt change in the lateral mobility of antibodies bound to the membrane of intact cells [see, e.g., Schroit and Pagano (1981)]. An interesting result of the temperature-dependent lateral diffusion measurements shown in Figure 5 is the small but significant shift of the phase transition temperature to higher temperatures upon addition of the anti-lipid hapten antibody. The observed temperature shift results most likely from lipid–protein and protein–protein interactions at the surface of the membrane. (The small change of the reporter lipid, from NBD-DMPE to the lipid hapten, is not expected to raise the transition temperature.) Interactions between neighboring proteins in two-dimensional antibody–lipid hapten clusters [or perhaps 2D antibody crystals (Uzgiris & Kornberg, 1983)] may be transmitted to the phospholipid acyl chains and may cause an increased ordering of the chains and the concomitant shift of the transition temperature. This mechanism suggests that at a certain critical temperature the binding of antibodies (or other effector molecules) can induce a lipid-phase transition and phase separation. It is at least conceivable that the transduction of signals across cytoplasmic membranes could occur via a localized lipid-mediated protein sorting mechanism.

Another important result of the experiments presented here is the relative insensitivity of the lateral diffusion coefficients on the antibody surface concentration. An old problem of lateral diffusion of membrane proteins is addressed here: Why do membrane proteins usually diffuse by about 2 orders of magnitude more slowly in cells than in model membranes? The proposed mechanisms for the observed reduction in the mobility of membrane proteins include interactions with cytoskeletal elements (Edelmann, 1976) and microviscosity increases due to high protein concentrations or protein aggregation. These models have been tested in several systems, however with partially contradictory results: When the cytoskeleton was disrupted mechanically or chemically, the lateral diffusion coefficients increased in some cases (Sheetz et al., 1980; Schindler et al., 1980; Tank et al., 1982) but not in others (e.g., surface immunoglobulins on lymphocytes; Henis and Elson, 1981). Also, when the cytoplasmic part of the EGF receptor was deleted by genetic engineering, the lateral diffusion coefficient was still very low and almost the same as that of the native receptor (Livneh et al., 1986). Finally, when the lipid-to-protein ratio was decreased in a model membrane system (reconstituted bacteriorhodopsin) down to 30 mol/mol, the protein lateral diffusion coefficient was restricted, but only by a factor of about 10 (Peters & Cherry, 1982). In the present study, an analogous experiment with a membrane surface protein instead of an integral membrane protein has been carried out. The results of the two experiments are qualitatively quite similar, although they differ quantitatively: The antibody lateral diffusion coefficient decreases only 2–3-fold when the antibody surface concentration is increased up to saturation. Thus, also in this system, the protein–protein interactions are not strong enough to cause a substantial reduction in the lateral mobility. Whether more highly glycosylated surface proteins exhibit stronger interactions is still an open question.

Lateral diffusion coefficients of antibodies bound to lipid haptens have been measured before in other model systems (Smith et al., 1979; Subramaniam & McConnell, 1986) and in cells (Schroit & Pagano, 1981). It is known from these studies that membrane-bound antibodies diffuse almost as rapidly as the lipids themselves in the fluid, liquid-crystalline phase. This observation is confirmed in the supported bilayer system. In fact, the measured diffusion coefficient of membrane-bound antibodies is about 2 times slower than that of the free lipids (Table I and Figure 5). This is expected if one assumes that (i) the antibody (IgG) bridges two phospholipids, (ii) the lipid haptens diffuse as two linked individual entities with friction coefficients that are not altered by the binding of antibody, and (iii) the friction of the antibody in the aqueous phase is negligable and does not contribute to the diffusion coefficient of the whole complex.[4] Then, the total friction coefficient of the complex is simply the sum of the friction coefficients of the two lipids

$$f = f_1 + f_2 = 2f_1 \tag{2}$$

and by use of Einstein's relation, the diffusion coefficient of the antibody becomes

$$D_{Ab} = \frac{kT}{f} = \frac{kT}{2f_1} = \frac{D_L}{2} \tag{3}$$

with D_L being the lateral diffusion coefficient of the lipid hapten.

The observation that the antibodies diffuse rapidly even at very high surface concentrations in supported bilayers is in apparent disagreement with a related study where monoclonal anti-nitroxide antibodies were bound to supported phospholipid monolayers on alkylated solid substrates (Subramaniam et al., 1986). The lateral diffusion of the bound antibodies became arrested on the supported monolayers at high incubation concentrations (100 $\mu g/mL$) when they were supported on solid substrates that were derivatized with long alkyl chains. Perhaps, the binding of high amounts of antibody induced a phase transition in supported monolayers too (as observed with supported bilayers) and caused the arrest of diffusion on monolayers with high antibody densities.

A few additional comments on supported phospholipid bilayers should be made: (1) In earlier work (Tamm &

[4] Proof that this last assumption is correct comes from the lateral diffusion coefficient of IgG in solution, which was measured to be 4.8×10^{-7} cm^2/s, which is about an order of magnitude faster than the lateral diffusion coefficients of lipids in membranes.

McConnell, 1985) it has been concluded that the phospholipids in supported phospholipid bilayers exhibit rapid lateral diffusion with mobile fractions that approach 100%. It is found here (Table I) that the phospholipid lateral diffusion coefficients and mobile fractions are somewhat reduced in supported bilayers if compared to those of multibilayers of the same lipid composition. (2) The phospholipid phase transition temperatures in supported bilayers as detected by lateral diffusion are a few degrees below the transition temperature detected in multibilayers by some other physical techniques, such as microcalorimetry [Tamm & McConnell (1985) and Figure 5]. (3) Data are presented here (Table I) which demonstrate that asymmetric supported phospholipid bilayers can be made and that the same lateral diffusion coefficients are measured whether the first, second, or both leaflets of the bilayer are labeled. In fact, all bilayers containing lipid hapten were asymmetric lipid bilayers. (4) Supported bilayers are stable for several days if kept under water or buffer. Only very small decreases in fluorescence intensities are observed after 3 days, and the lateral diffusion coefficients and mobile fractions are essentially unaltered (data not shown). (5) An exchange of the surrounding water by buffer with mono- and bivalent cations does not change either the integrity or the diffusion behavior of the supported bilayers.

The potential uses of supported phospholipid bilayers are widespread and range from strictly physical–chemical measurements to investigation of pending problems in cell biology and immunology. Certainly, it seems to be the model membrane of choice for the measurement of lateral diffusion coefficients of surface-bound membrane proteins (as shown here) and also of lipid-anchored membrane proteins that have been found recently in lymphocytes, protozoa, and other cells. It will be interesting to follow binding reactions with supported bilayers and to study molecular interactions with the surfaces of single cells.

Acknowledgments

I thank Prof. G. Köhler for the generous gift of the hybridoma cell line GK14-1 and various antibody samples. I also thank I. Bartoldus for her skillful technical assistance, Dr. G. Hänisch and his workshop for their competent help in developing our FRAP instrument, and E. Aebischer for typing the manuscript.

Registry No. DMPC, 18194-24-6; POPC, 26853-31-6.

References

Criado, M., Vaz, W. L. C., Barrantes, F. J., & Jovin, T. M. (1982) *Biochemistry 21*, 5750–5755.

Douillard, J. Y., & Hoffmann, T. (1983) *Methods Enzymol. 92*, 168–174.

Edelman, G. M. (1976) *Science (Washington, D.C.) 192*, 218–226.

Forni, L. (1979) in *Immunological Methods* (Lefkovits, I., & Pernis, B., Eds.) Vol. 1, pp 151–167, Academic, New York.

Fromherz, P. (1975) *Rev. Sci. Instrum. 46*, 1380–1385.

Gaupp, H., Maeder, M., & Zuberbühler, A. (1980) *Talanta 27*, 1037–1045.

Goding, J. W. (1983) *Monoclonal Antibodies: Principles and Practice*, pp 115–116, Academic, London.

Hafeman, D. G., von Tscharner, V., & McConnell, H. M. (1981) *Proc. Natl. Acad. Sci. U.S.A. 78*, 4552–4556.

Hänggi-Mojtabai, F. (1985) Diss. phil. II, University of Basel.

Henis, Y. I., & Elson, E. L. (1981) *Proc. Natl. Acad. Sci. U.S.A. 78*, 1072–1076.

Kiefer, M. (1979) in *Immunological Methods* (Lefkovits, I., & Pernis, B., Eds.) Vol. 1, pp 137–150, Academic, New York.

Kleemann, W., & McConnell, H. M. (1976) *Biochim. Biophys. Acta 419*, 206–222.

Laemmli, U. K. (1970) *Nature (London) 227*, 680–685.

Livneh, E., Benverniste, M., Prywes, R., Felder, S., Kam, Z., & Schlessinger, J. (1986) *J. Cell Biol. 103*, 327–331.

Lösche, M., Sackmann, E., & Möhwald, H. (1983) *Ber. Bunsen-Ges. Phys. Chem. 87*, 848–852.

Lowry, O. H., Rosebrough, N. J., Farr, A. L., & Randall, R. J. (1951) *J. Biol. Chem. 193*, 265–275.

McConnell, H. M., Tamm, L. K., & Weis, R. M. (1984) *Proc. Natl. Acad. Sci. U.S.A. 81*, 3249–3253.

McConnell, H. M., Watts, T. H., Weis, R. M., & Brian, A. A. (1986) *Biochim. Biophys. Acta 864*, 95–106.

Peters, R., & Cherry, R. J. (1982) *Proc. Natl. Acad. Sci. U.S.A. 79*, 4317–4321.

Rubenstein, J. L. R., Smith, B. A., & McConnell, H. M. (1979) *Proc. Natl. Acad. Sci. U.S.A. 76*, 15–18.

Schindler, M., Koppel, D. E., & Sheetz, M. P. (1980) *Proc. Natl. Acad. Sci. U.S.A. 77*, 1457–1461.

Schroit, A. J., & Pagano, R. E. (1981) *Cell (Cambridge, Mass.) 23*, 105–112.

Sheetz, M. P., Schindler, M., & Koppel, D. E. (1980) *Nature (London) 285*, 510–512.

Smith, B. A., & McConnell, H. M. (1978) *Proc. Natl. Acad. Sci. U.S.A. 75*, 2759–2763.

Smith, L. M., Parce, J. W., Smith, B. A., & McConnell, H. M. (1979) *Proc. Natl. Acad. Sci. U.S.A. 76*, 4177–4179.

Subramaniam, S., Seul, M., & McConnell, H. M. (1986) *Proc. Natl. Acad. Sci. U.S.A. 83*, 1169–1173.

Tamm, L. K., & McConnell, H. M. (1985) *Biophys. J. 47*, 105–113.

Tank, D. W., Wu, E.-S., & Watt, W. W. (1982) *J. Cell Biol. 92*, 207–212.

Thompson, T. E., & Tillack, T. W. (1985) *Annu. Rev. Biophys. Bioeng. 14*, 361–386.

Uzgiris, E. E., & Kornberg, R. D. (1983) *Nature (London) 301*, 125–129.

Vaz, W. L. C., & Hallmann, D. (1983) *FEBS Lett. 152*, 287–290.

von Tscharner, V., & McConnell, H. M. (1981) *Biophys. J. 36*, 409–419.

Wu, E.-S., Jacobson, K., & Papahadjopoulos, D. (1977) *Biochemistry 16*, 3936–3941.